

Syntheses, Structures, and Luminescence of $\text{H}_4\text{BTC}_4\text{A}\cdot\text{CH}_3\text{OH}$ and $[\text{Ag}(\text{PPh}_3)_4](\text{H}_3\text{BTC}_4\text{A})\cdot\text{DMF}$ ($\text{H}_4\text{BTC}_4\text{A} = p\text{-}tert\text{-Butylthiacalix[4]arene}$)

S. B. Sun^a, Y. J. Dong^a, X. L. Lai^b, Z. Y. Yuan^a, H. Zhang^a, J. L. Xie^a, L. S. Wang^a, ^{*}, and P. X. Lei^a, ^{**}

^a Hubei Provincial Key Laboratory of Green Materials for Light Industry, Collaborative Innovation Center of Green Light-Weight Materials and Processing, School of Material and Chemical Engineering, Hubei University of Technology, Wuhan, 430068 P.R. China

^b CNOOC Tianjin Chemical Research and Design Institute Limited Corporation, Tianjin, 300131 P.R. China

^{*}e-mail: wangls@mail.hbut.edu.cn

^{**}e-mail: leipx@mail.hbut.edu.cn

Received August 29, 2022; revised December 11, 2022; accepted December 15, 2022

Abstract—One inclusion complex $\text{H}_4\text{BTC}_4\text{A}\cdot\text{CH}_3\text{OH}$ (**I**) and one ionic complex $[\text{Ag}(\text{PPh}_3)_4](\text{H}_3\text{BTC}_4\text{A})\cdot\text{DMF}$ (**II**) ($\text{H}_4\text{BTC}_4\text{A} = p\text{-}tert\text{-butylthiacalix[4]arene}$) were obtained through solvothermal reaction. Their structures were determined by single crystal X-ray diffraction (CCDC nos. 2203699 (**I**) and 2203700 (**II**)), and further evidenced by FT-IR, ¹H NMR, UV–Vis spectra, elemental analyses and so on. For complex **I**, there is one molecule of $\text{H}_4\text{BTC}_4\text{A}$ in the asymmetric unit cell, in whose cavity one guest molecule of methanol was included. In the asymmetric unit of complex **II**, there are one cation of $[\text{Ag}(\text{PPh}_3)_4]^+$, one deprotonated thiocalix[4]arene anion of $[\text{H}_3\text{BTC}_4\text{A}]^-$ and one DMF solvent molecule. Upon the irradiation of UV light in their acetonitrile solution, complex **I** demonstrate an emission at 294 nm, and $[\text{Ag}(\text{P}(\text{Ph}_3)_4)]\text{NO}_3$ show an emission at 304 nm. Complex **II** not only showed the characteristic strong emissions of complex **I** (294 nm) and $[\text{Ag}(\text{P}(\text{Ph}_3)_4)]\text{NO}_3$ (305 nm), but also produced a new weak emission at 368 nm, which further verified the formation of complex **II**.

Keywords: calixarene, silver, luminescence, inclusion, ionic compound

DOI: 10.1134/S107032842370046X

INTRODUCTION

Calixarenes, the third generation of supramolecular hosts, are a class of macrocyclic compounds consisting of several para-substituted phenols connected by the bridges of methylene groups or sulfur atoms to form cyclic oligomers. They are a kind of good molecular vessels to accommodate organic molecules or inorganic metal ions owing to their unique bowl-like structure with adjustable sizes and cavities [1]. The research on calixarenes has received growing attentions owing to their extensive applications in the fields of sensors, materials, coordination chemistry, molecular recognition, electrode material and so on [2]. Especially in the field of coordination chemistry, calix[4]arenes, as multidentate chelating ligands, can be easily chelated with transition metal ions, non-transition metal ions to form the coordination complexes of MC_4A [3] and $\text{M}_2\text{C}_4\text{A}$ [4], or their aggregations [5, 6]. Thiocalixarenes and their derivatives are a kind of calixarenes containing bridging sulfur atoms [7], the flexible C–S bond lengths and C–S–C bond angles not only render them to accommodate bigger guest molecules, but also afford them stronger coordi-

nation abilities compared to those calixarenes bridged by the methylene group. To date, many guest molecules of H_2O , pyridine [8], CH_2Cl_2 [9], CHCl_3 [10], $\text{CH}_2\text{ClCH}_2\text{Cl}$ [11], CH_3NO_2 , CH_3CN [12] and so on, have been included in thiocalix[4]arene. Moreover, thiocalix[4]arene are easily chelated with transition metal ions to form the secondary building block of $\text{M}_4\text{C}_4\text{A}$ [13] besides the building blocks of $\text{M}_2\text{C}_4\text{A}$ [14] and MC_4A [15]. These building blocks can further form sandwich-like cluster [16, 17], wheel-like cluster [18], $[\text{Co}_{24}]$ metallamacrocyclic [19], $[\text{Co}_{32}]$ nanosphere [20], and cationic nanocage of $[\text{Mn}_{24}]$ [21]. It is notable that the shuttlecock-like building blocks of $\text{M}_4\text{C}_4\text{A}$ can be bridged by dicarboxylic acid [22, 23] or tricarboxylic acid [24] to form a series of nanoscale polyhedral coordination cages with different sizes and shapes.

Compared to the extensive research on the coordination chemistry of calixarenes [25] and thiocalixarenes [26], the ionic compounds of calixarene have been less explored beside the species of calix[n]arene–sulphonic acid ($n = 4, 6, 8$), which can readily form

ionic compounds or coordination compounds [27] owing to the presence of sulfonic acid group. Only a few ionic salts of calixarene without sulphonate functional group have been reported up to now. For example, Katsuaki et al. reported the ionic complexes consisting of Keggin anions and calix[4]arene- Na^+ [28]. White et al. had synthesized a series of salt of alkali metal and triethylamine of thiocalix[4]arene [10]. Limberg et al. had reported a series of tetraphenylphosphonium salt based on the anionic clusters of calixarene and vanadium, which demonstrated oxidative activity on alcohol [29]. Therefore, the research on the ionic compounds of calixarene is a promising yet less explored field.

During our research on the assembly of thiocalix[4]arenes, we had obtained one inclusion complex of $\text{H}_4\text{BTC}_4\text{A}\cdot\text{CH}_3\text{OH}$ (**I**) and one ionic compound $[\text{Ag}(\text{PPh}_3)_4](\text{H}_3\text{BTC}_4\text{A})$ (**II**). Herein, we reported their syntheses, crystal structures, characterizations and luminescence features.

EXPERIMENTAL

Materials and methods. *p*-tert-Butylthiocalix[4]arene ($\text{H}_4\text{BTC}_4\text{A}$) was prepared according to the reported literature [9]. Other materials were obtained commercially. They were of analytical reagent grade and used as received without further purification. ^1H NMR spectra were recorded on a Mercury 300 spectrometer operating at 300 MHz. Mass spectrometric (MS) measurements performed by a direct-exposure probe using electron impact ionization (EI) were made on a VG 70S instrument. FT-IR spectra were recorded within the 400–4000 cm^{-1} region on a Perkin Elmer Spectrum 100 FT-IR spectrometer. UV–Vis spectra were collected on Shimadzu UV Probe 2700. Luminescent spectra were recorded on a Cary Eclipse Spectrofluorometer.

Synthesis of $\text{CH}_3\text{OH}\subset\text{H}_4\text{BTC}_4\text{A}$ ($\text{H}_4\text{BTC}_4\text{A}\cdot\text{CH}_3\text{OH}$) (I**).** To a mixed solvent of DMF– CH_3OH (8 mL, 1 : 1), $\text{H}_4\text{BTC}_4\text{A}$ (0.0386 g, 0.0536 mmol), 4,4'-bipyridine (0.0546 g, 0.0350 mmol) and AgNO_3 (0.0344 g, 0.202 mmol) was added, then 0.25 mL Et_3N was followed. The mixture was stirred for half an hour and sealed in a 20-mL Teflon-lined autoclave, which are then kept at 130°C for three days and slowly cooled to 20°C at a rate of about 4°C/h. The obtained mixture was filtered to give a light-yellow filtrate, which was left undisturbedly, then lots of colorless plate crystals, were obtained after volatilization of the solvent. The yield was 0.0147 g (38.0%).

For $\text{C}_{41}\text{H}_{52}\text{O}_5\text{S}_4$
Anal. calcd., % C, 65.21 H, 7.13
Found, % C, 65.39 H, 6.96

FT-IR (KBr pellet; ν , cm^{-1}): 3422 v.s, 3259 s, 2964 s, 1639 m, 1477 w, sh, 1457 w, 1384 s, 1269 w, 1245 w, 1209 m, 1093 s, 984 w, 889 m, 859 m, 753 m, 742 s, 585 m. ^1H NMR (DMSO-d_6 , 300 K): 7.52 (s, 8H, Ar–H), 1.16 (s, 36H, $-\text{C}(\text{CH}_3)_3$).

Synthesis of $[\text{Ag}(\text{PPh}_3)_4](\text{H}_3\text{BTC}_4\text{A})\cdot\text{DMF}$ (II**).** To a mixed solvent of DMF– CH_3OH (8 mL, 1 : 1), $\text{H}_4\text{BTC}_4\text{A}$ (0.0386 g, 0.0536 mmol), triphenylphosphine (0.0546 g, 0.0350 mmol) and AgNO_3 (0.0354 g, 0.208 mmol) were added, then followed by 0.25 mL Et_3N . The mixture was stirred for half an hour was sealed in a 20-mL Teflon-lined autoclave, which were then kept at 130°C for three days and slowly cooled to 20°C at a rate of about 4°C/h. The obtained mixture was filtered to give a light-yellow filtrate, which were left undisturbedly, then lots of colorless plate crystals, were obtained after volatilization of the solvent. The yield was 0.008 g (43% based on PPh_3).

For $\text{C}_{115}\text{H}_{114}\text{AgO}_5\text{P}_4\text{S}_4\text{N}$

Anal. calcd., %	C, 70.82	H, 5.89	N, 0.72
Found, %	C, 70.96	H, 6.02	N, 0.68

FT-IR (KBr pellet; ν , cm^{-1}): 3415 s, w, 1639 m, 1478 m, 1434 m, 1384 s, 1339 m, 1308 w, 1090 s, 984 w, 859 w, 744 w, 695 m, 543 m, 517 m, 499 m. ^1H NMR (DMSO-d_6 , 300 K): 7.95 s, 1H, $-\text{CHO}$, 7.52 (s, 8H, Ar–H), 7.40 (d, 36H, Ar–H), 7.25 (d, 24H, Ar–H), 2.89 (s, 3H, $-\text{NCH}_3$), 2.73 (s, 3H, $-\text{NCH}_3$), 1.16 (s, 36H, $-\text{C}(\text{CH}_3)_3$).

X-ray structure determination. Single crystal X-ray diffraction data of both compounds were collected on a Bruker SMART APEX CCD diffractometer with graphite monochromated CuK_α radiation ($\lambda = 1.54184 \text{ \AA}$) by an ω -scan mode at low temperature of 150(2) K. Crystal structures were solved by direct methods (SHELXS2014) [30] and refined by full-matrix least squares on F^2 with anisotropic thermal parameters for all non-hydrogen atoms (SHELXL2014) [31]. All hydrogen atoms were assigned on the calculated positions. Disordered atoms are restrained with reasonable bond lengths. Those calculations were performed on a PC with OLEX2 program. Crystallographic data and structure refinement information for both complexes are summarized in Table 1. Selected bond lengths, bond angles and hydrogen bonding lists of both complexes are listed in Table 2 and Table 3, respectively.

RESULTS AND DISCUSSIONS

Single crystal X-ray diffraction structural analysis reveals that compound **I** ($\text{H}_4\text{BTC}_4\text{A}\cdot\text{CH}_3\text{OH}$) crystallizes in tetragonal system, $P\bar{4}2_1c$ space group. As shown in Fig. 1a, there is one $\text{H}_4\text{BTC}_4\text{A}$ molecule and one methanol solvent molecule in the asymmetric unit

Table 1. Crystallographic data and structure refinement information for complexes **I** and **II**

Parameter	Value	
	I	II
Empirical formula	C ₄₁ H ₅₂ O ₅ S ₄	C ₁₁₅ H ₁₁₄ O ₅ S ₄ P ₄ Ag
Formula weight	753.06	1950.06
Wavelength, Å	1.54184	1.54184
Crystal system	Tetragonal	Triclinic
Space group	<i>P</i> 4 ₂ 1 <i>c</i>	<i>P</i> 1
<i>a</i> , Å	22.2668(3)	13.9393(3)
<i>b</i> , Å	22.2668(3)	14.3873(2)
<i>c</i> , Å	17.6767(4)	27.5688(7)
α, deg	90	81.8891(18)
β, deg	90	76.479(2)
γ, deg	90	89.1770(16)
<i>V</i> , Å ³	8764.3(3)	5320.9(2)
<i>Z</i>	8	2
ρ, g/cm ³	1.141	1.217
<i>F</i> (000)	3216	2044
Crystal size, mm	0.32 × 0.25 × 0.23	0.35 × 0.26 × 0.23
Goodness-of-fit on <i>F</i> ²	1.035	1.041
Reflections collected/unique	24037/7516	58302/18974
<i>R</i> ₁ , <i>wR</i> ₂ (<i>I</i> > 2σ(<i>I</i>))*	<i>R</i> ₁ = 0.0931, <i>wR</i> ₂ = 0.2540	<i>R</i> ₁ = 0.0667, <i>wR</i> ₂ = 0.1796
<i>R</i> ₁ , <i>wR</i> ₂ (all data)**	<i>R</i> ₁ = 0.1139, <i>wR</i> ₂ = 0.2874	<i>R</i> ₁ = 0.0779, <i>wR</i> ₂ = 0.1919
Residual electron density (min/max), e/Å ³	−0.309, 0.941	−1.05, 1.44

* $R_1 = \Sigma |F_o| - |F_c| / \Sigma |F_o|$, ** $wR_2 = \{\Sigma [w(F_o^2 - F_c^2)^2] / \Sigma [w(F_o^2)^2]\}^{1/2}$.

Table 2. Selected bond lengths (Å) and bond angles (deg) of compound **I** and **II**

Bond length	<i>d</i> , Å	Bond angle	ω, deg
C—O	1.331(10)–1.378(9)	I C—S—C	100.7(4)–101.8(4)
C—S	1.768(8)–1.800(8)		
Ag—P	2.6238(9)–2.6533(11)	II Ag—P—Ag C—S—C	107.98(3)–111.25(3) 100.47(19)–108.2(2)
C—O	1.317(5)–1.348(6)		
C—S	1.774(6)–1.785(4)		

cell. In the molecule of H₄BTC₄A, four *p*-*tert*-butyl-phenols are linked by four bridged sulfur atoms to form a shuttlecock-like ring. There are position disorders in two *tert*-butyl groups owing to the rotation of *tert*-butyl group. The C—S bond lengths are in the range of 1.763(8)–1.801(8) Å, which are longer than that of carbon-sulfur double bond (1.70 Å) but shorter than that of carbon-sulfur single bond (1.82 Å) owing to the *p*–π conjugative effect between the sulfur atom and the

phenyl ring. The C—O bond length is in the range of 1.333(10)–1.388(9) Å. One methanol molecule is included in the cavity of H₄BTC₄A to form an inclusion complex. It is notable that the methyl group was pointing to the hydrophilic cavity and the hydroxyl group was pointing the outside of the H₄BTC₄A. At the lower rim of H₄BTC₄A (Fig. 2a), there are two intramolecular hydrogen bonds between adjacent phenolic hydroxyl groups: O(1)–H(1A)···O(3)

Table 3. Hydrogen bond lengths (Å) and bond angles (deg) of compound **I** and **II**

D—H...A	Distance, Å			\angle DHA, deg
	D—H	H...A	D...A	
I				
O(1)—H(1A)...O(3)	0.84	2.11	2.947(10)	178.4
O(2)—H(2A)...O(3)	0.84	2.06	2.904(10)	178.1
II				
O(2)—H(2)...O(3)	0.90(1)	1.74(3)	2.601(5)	156(7)
O(4)—H(4)...O(3)	0.86(7)	1.69(7)	2.519(5)	163(7)

(2.947(10) Å, 178.4°) and O(2)—H(2A)…O(3) (2.904(10) Å, 178.1°).

Single-crystal X-ray structural analysis reveals that compound **II** ($[\text{Ag}(\text{P}(\text{C}_6\text{H}_5)_3)_4]\text{[H}_3\text{BTC}_4\text{A}]\cdot\text{DMF}$) crystallizes in triclinic system, $P\bar{1}$ space group. As shown in Fig. 1b, there are one cation of $[\text{Ag}(\text{P}(\text{C}_6\text{H}_5)_3)_4]^+$, one deprotonated thiocalix[4]arene anion of $[\text{H}_3\text{BTC}_4\text{A}]^-$ and one DMF solvent molecule in the asymmetric unit of compound **II**. In the cation of $[\text{Ag}(\text{P}(\text{C}_6\text{H}_5)_3)_4]^+$, the silver ion is coordinated with four phosphorus atoms from triphenylphosphine ligands to form a slightly distorted tetrahedron with the Ag—P bond lengths falling between 2.6244(9)–2.6533(9) Å. The bond angles of PAgP are ranged from 107.98(3)° to 111.25(3)°, which are slightly deviated from 109°28', further confirming the distorted nature of the AgP₄ tetrahedron. The deprotonated thiocalix[4]arene anion showed a structure similar to that of compound **I** except that one proton of thiocalix[4]arene was lost. The C—S bond length of 1.777(6)–1.786(5) Å and the C—O bond length of 1.316(5)–1.351(6) Å, were found slightly shorter than those of free ligand of $[\text{H}_4\text{BTC}_4\text{A}]$. One DMF solvent molecule is included as a guest molecule in the cavity of $[\text{H}_3\text{BTC}_4\text{A}]^-$. At the lower rim of $\text{H}_4\text{BTC}_4\text{A}$, there are two intermolecular hydrogen bonds between adjacent phenolic hydroxyl groups (Fig. 2b): O(4)—H(4)…O(3) (2.519(5) Å, 163(7)°) and O(2)—H(2)…O(3) (2.601(5) Å, 156(7)°).

Cell packing diagram of compound **I** is shown in Fig. 3a. Those molecules of $\text{H}_4\text{BTC}_4\text{A}$ are packed along the ab plane to form a 2D layer. The cavities of those $\text{H}_4\text{BTC}_4\text{A}$ are parallel to the *c* axis to form a channel, which accommodates the guest methanol molecules. Cell packing diagram of compound **II** is shown in Fig. 3b. The anion layer and the cation layer of $[\text{Ag}(\text{P}(\text{C}_6\text{H}_5)_3)_4]^+$ are packed along the *c* axis in a staggered way. The anion layer along the ab plane consists of two layers of $[\text{H}_3\text{BTC}_4\text{A}]^-$, the hydrophilic low rims are facing the cation layer, while the hydrophobic upper rims are facing with each other.

In the infrared spectrum of compound **I**, there is a strong and broad absorption band around 3500 cm^{−1},

which stems from the stretching vibration of the hydroxyl functional group on the ligand of thiocalix[4]arene. The strong absorption peaks at 2960–2870 cm^{−1} are attributed to the anti-symmetric/symmetric stretching vibration of *t*-butyl. The three peaks at 1600–1500 cm^{−1} are corresponded to the skeleton vibration of benzene ring. The peaks at 840, 750 and 670 cm^{−1} are the characteristic absorption of para-substituted benzene in the main ligand thiocalix[4]arene. In the infrared spectrum of compound **II**, the broad strong absorption band around 3400 cm^{−1} is assigned to the stretching vibration of —OH of the thiocalix[4]arene ligand. The anti-symmetric/symmetric stretching vibrations of *t*-butyl are not obvious owing to the overlap of the hydroxyl peak. The peak at ca. 1639 cm^{−1} corresponds to the skeleton vibration of benzene ring. The peaks at 840, 750 and 670 cm^{−1} are the characteristic absorption of para-substituted benzene in the main ligand thiocalix[4]arene.

$[\text{Ag}(\text{PPh}_3)_4]\text{NO}_3$ is prepared according to literature for comparing its spectral properties [32]. UV–Vis, luminescent spectra of $[\text{Ag}(\text{PPh}_3)_4]\text{NO}_3$, compounds **I** and **II** were studied in the acetonitrile solution with a concentration of ca. 1.0×10^{-5} g L^{−1} (Notation: complex **I** is slightly soluble in the acetonitrile solvent, and the concentration of complex **I** at such a low level was just calculated according to its weight without further measurement). As shown in Fig. 4a, $[\text{Ag}(\text{PPh}_3)_4]\text{NO}_3$ shows a strong absorption band about 213 nm (E_2 band of triphenylphosphine) and a medium absorption band about 260 nm (E_2 band of triphenylphosphine). Due to its poor solubility in acetonitrile, compound **I** (Notation: the methanol molecule included in the cavity of thiocalix[4]arene was possibly exchanged by acetonitrile molecule in the test condition) shows a strong absorption band at about 203 nm (E_1 band of $\text{H}_4\text{BTC}_4\text{A}$), a medium absorption band around ca. 277 nm (E_2 band of $\text{H}_4\text{BTC}_4\text{A}$) and a weak absorption band at about 305 nm (B band of $\text{H}_4\text{BTC}_4\text{A}$). Compound **II** shows a strong absorption band about 210 nm, a weak absorption band about 260 nm and a weak absorption band about 305 nm, which demonstrate the typical absorption band of $[\text{Ag}(\text{PPh}_3)_4]\text{NO}_3$.

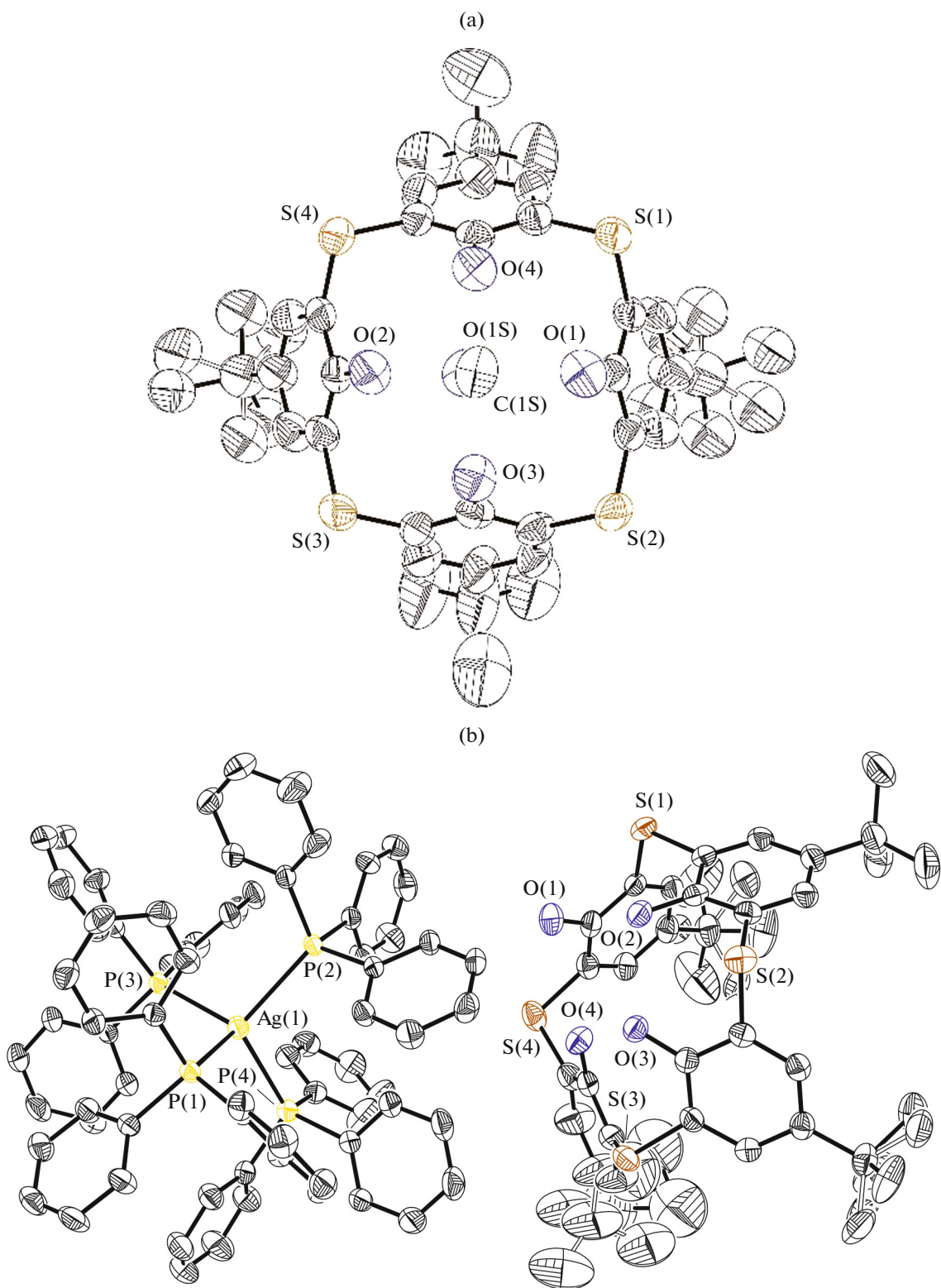


Fig. 1. ORTEP diagrams of compounds **I** (a) and **II** (b) with thermal ellipsoids at 40% level. Hydrogen atoms were omitted for clarity.

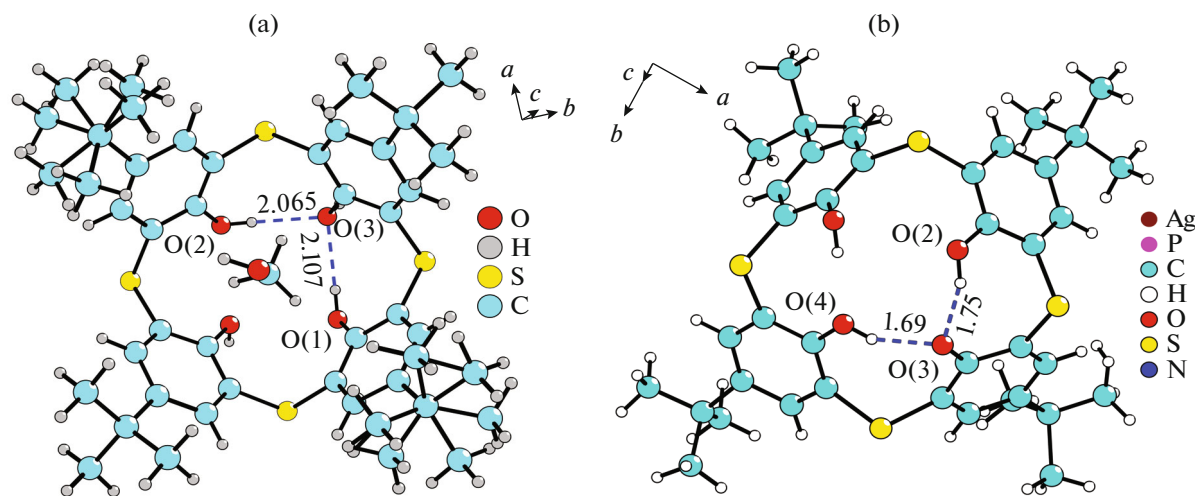


Fig. 2. Hydrogen bonding diagram of compound I (a) and II (b).

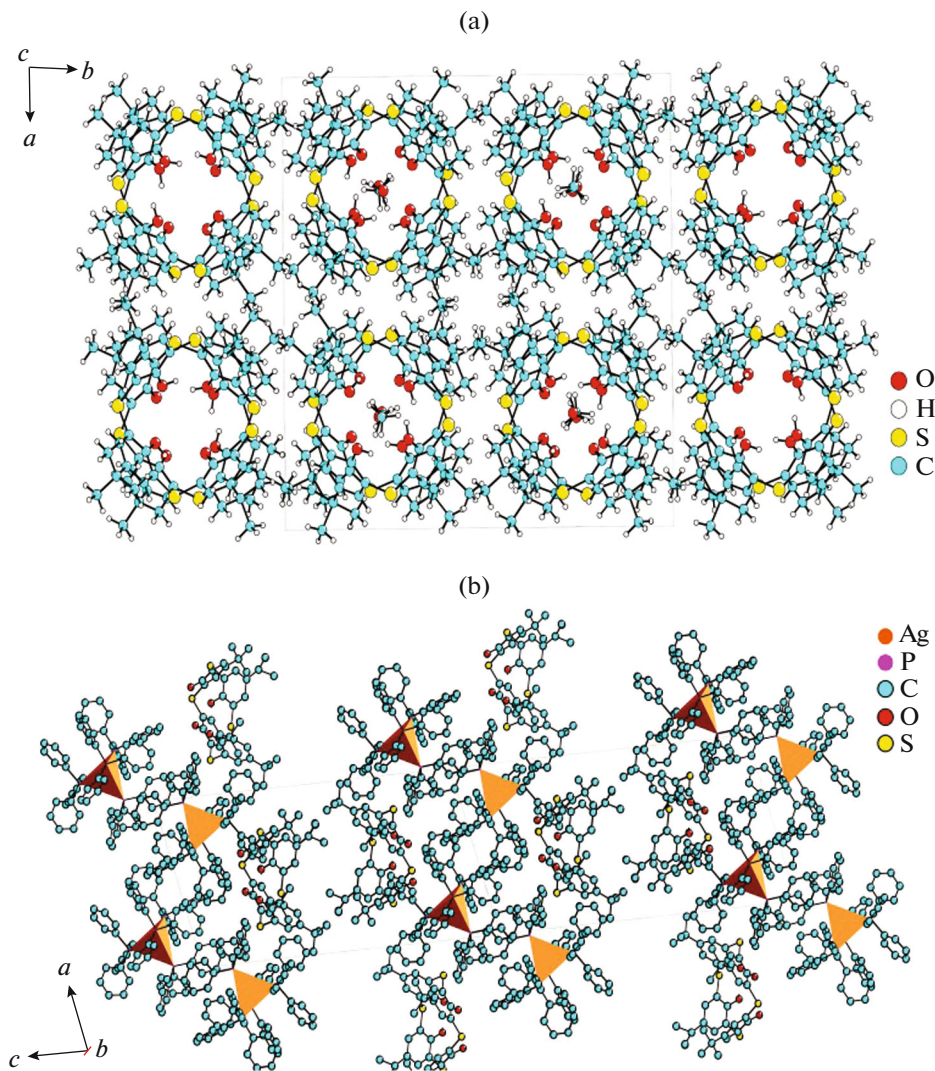


Fig. 3. Cell packing diagram of compound I along the *ab* plane (a); cell packing diagram of compound II along the *ac* plane (b).

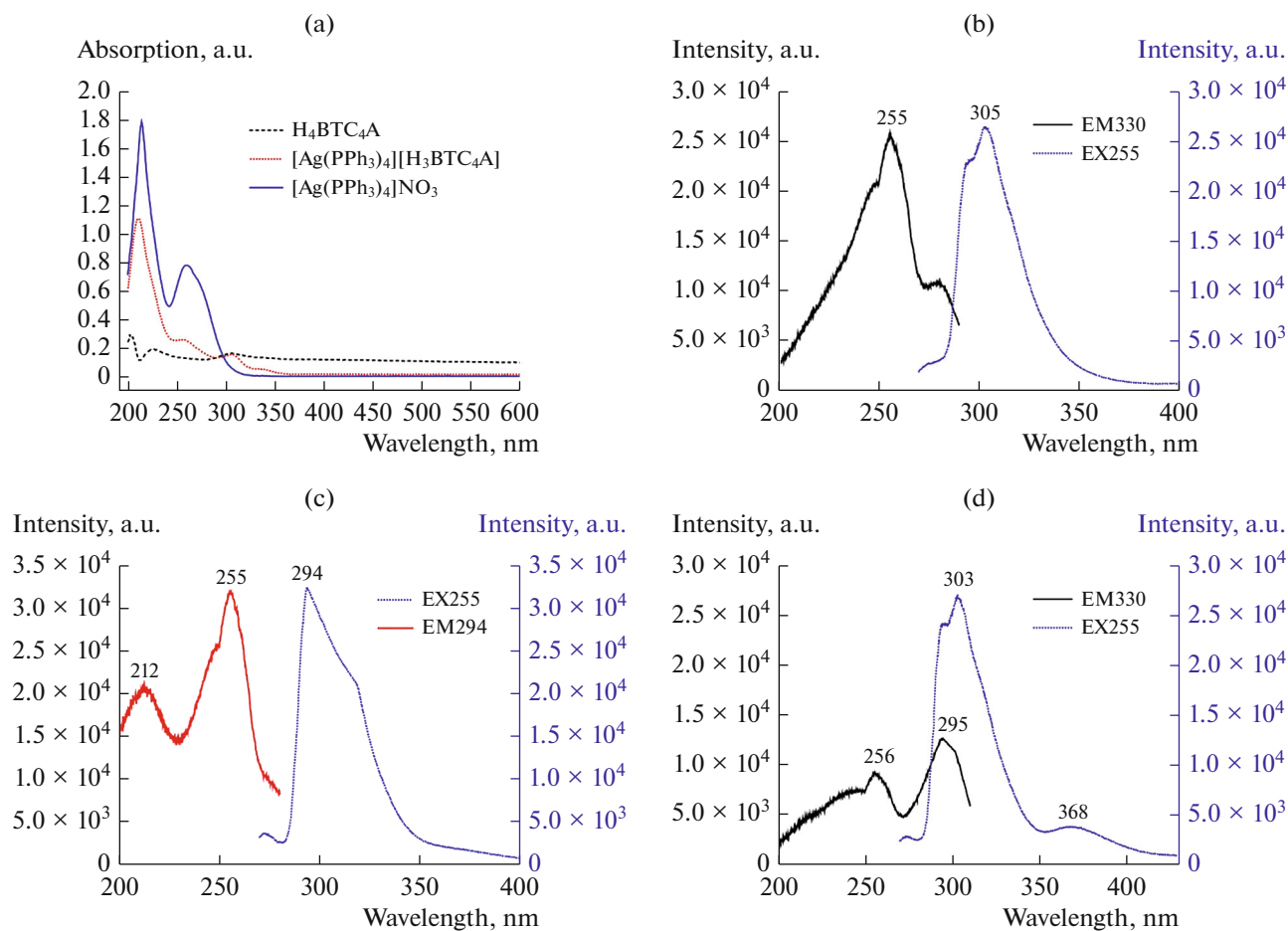


Fig. 4. UV–Vis diagram of $[\text{Ag}(\text{PPh}_3)_4]\text{NO}_3$, compounds **I** and **II** in their acetonitrile solutions with the concentration of ca. $1.0 \times 10^{-5} \text{ mol L}^{-1}$ (a); excitation spectrum and emission spectrum of $[\text{Ag}(\text{PPh}_3)_4]\text{NO}_3$ (b), compound **I** (c) and compound **II** (d).

then confirms that compound **II** contains the cation of $[\text{Ag}(\text{PPh}_3)_4]^+$ and the anion of $[\text{H}_4\text{BTC}_4\text{A}]^-$.

Photoluminescence (PL) properties of $[\text{Ag}(\text{PPh}_3)_4]\text{NO}_3$, compounds **I** and **II** were explored using their acetonitrile solutions with a concentration of ca. $1.0 \times 10^{-5} \text{ mol L}^{-1}$. As shown in Figs. 4b–4c, $[\text{Ag}(\text{PPh}_3)_4]\text{NO}_3$ demonstrates a strong emission band around 305 nm upon the excitation of 255 nm, and compound **I** shows a strong emission about 294 nm upon the same excitation. As for compound **II**, upon excitation at the same wavelength, it not only shows both characteristic strong emissions of $[\text{Ag}(\text{PPh}_3)_4]\text{NO}_3$ (303 nm) and compound **I** (295 nm), but also exhibits a weak emission at around 368 nm, which further proves the formation of $[\text{Ag}(\text{PPh}_3)_4](\text{H}_3\text{BTC}_4\text{A})$.

In summary, one inclusion compound of $\text{H}_4\text{BTC}_4\text{A} \cdot \text{CH}_3\text{OH}$ (**I**) and one new ionic compound of $[\text{Ag}(\text{PPh}_3)_4](\text{H}_3\text{BTC}_4\text{A})$ (**II**) were obtained by the solvothermal synthetic technique. Their structures were determined by single crystal X-ray diffraction, and further evidenced by FT-IR, UV–Vis spectra, and CHN analysis. Compound **I** demonstrates typical

molecular structure of thiocalix[4]arenes with one methanol molecule included in its cavity. Compound **II** possesses a cation of $[\text{Ag}(\text{P}_6\text{H}_5)_4]^+$ and one deprotonated calixarene anion of $[\text{H}_3\text{BTC}_4\text{A}]^-$. Upon the excitation at 255 nm, compound **I** demonstrates a strong emission at about 294 nm, while compound **II** shows strong characteristic emissions of $\text{H}_4\text{BTC}_4\text{A}$ (295 nm) and $[\text{Ag}(\text{PPh}_3)_4]\text{NO}_3$ (303 nm) and a weak new emission at 368 nm, indicating that they are a kind of potential luminescent materials.

ACKNOWLEDGMENTS

We thank the financial support of the National Natural Science Foundation of China (21101062), Science and Technology Department of Hubei Province (2014CFB600), Youth Chutian Scholar Fund of Hubei Province (4032401), State Key Laboratory of Structural Chemistry (20180023), Hubei Provincial Key Laboratory of Green Materials for Light Industry (201907A09).

CONFLICT OF INTEREST

The authors declare that they have no conflicts of interest.

REFERENCES

1. Gutsche, C.D., *Calixarenes: An Introduction*, Cambridge: Royal Society of Chemistry, 2008, 2nd ed.
2. Gutsche, C.D., *Encyclopedia of Supramolecular Chemistry*, New York: Marcel Dekker, Inc, 2004.
3. Corazza, F., Floriani, C., Chiesi-Villa, A., and Rizzolli, C., *Inorg. Chem.*, 1991, vol. 30, p. 4465.
4. McBurnett, B.G. and Cowley, A.H., *Chem. Commun.*, 1999, p. 17.
5. Chisholm, M.H., Folting, K., Streib, W.E., and Wu, D.-D., *Chem. Commun.*, 1998, p. 379.
6. Taylor, S.M., McIntosh, R.D., Beavers, C.M., et al., *Chem. Commun.*, 2011, vol. 47, no. 5, p. 1440.
7. Morohashi, N., Narumi, F., Iki, N., et al., *Chem. Rev.*, 2006, vol. 106, p. 5291.
8. Hong, J., Yang, C., Li, Y., et al., *J. Mol. Struct.*, 2003, vol. 655, no. 3, p. 435.
9. Akdas, H., Bringel, L., Graf, E., et al., *Tetrahedron Lett.*, 1998, vol. 39, p. 2311.
10. Bilyk, A., Hall, A.K., Harrowfield, J.M., et al., *Inorg. Chem.*, 2001, vol. 40, p. 672.
11. Iki, N., Kabuto, C., Fukushima, T., et al., *Tetrahedron*, 2000, vol. 56, p. 1437.
12. Arduini, A., Nachtigall, F.F., Pochini, A., et al., *Supramol. Chem.*, 2000, vol. 12, no. 3, p. 273.
13. Mislin, G., Graf, E., Hosseini, M.W., et al., *Chem. Commun.*, 1999, p. 373.
14. Morohashi, N., Hattori, T., Yokomakura, K., et al., *Tetrahedron Lett.*, 2002, vol. 43, p. 7769.
15. Asfari, Z., Bilyk, A., Dunlop, J.W.C., et al., *Angew. Chem. Int. Ed.*, 2001, vol. 40, no. 4, p. 721.
16. Sanz, S., Ferreira, K., and McIntosh, R.D., et al., *Chem. Commun.*, 2011, vol. 47, no. 32, p. 9042.
17. Xiong, K., Jiang, F., Gai, Y., et al., *Inorg. Chem.*, 2012, vol. 51, no. 5, p. 3283.
18. Kajiwara, T., Wu, H., Ito, T., et al., *Angew. Chem. Int. Ed.*, 2004, vol. 43, no. 14, p. 1832.
19. Bi, Y., Xu, G., Liao, W., et al., *Chem. Commun.*, 2010, vol. 46, no. 34, p. 6362.
20. Bi, Y., Wang, X.-T., Liao, W., et al., *J. Am. Chem. Soc.*, 2009, vol. 131, p. 11650.
21. Xiong, K.C., Jiang, F.L., Gai, Y.L., et al., *Chem. Eur. J.*, 2012, vol. 18, no. 18, p. 5536.
22. Xiong, K., Jiang, F., Gai, Y., et al., *Chem. Sci.*, 2012, vol. 3, no. 7, p. 2321.
23. Wang, S., Gao, X., Hang, X., et al., *J. Am. Chem. Soc.*, 2016, vol. 138, no. 50, p. 16236.
24. Liu, M., Liao, W., Hu, C., et al., *Angew. Chem. Int. Ed.*, 2012, vol. 51, no. 7, p. 1585.
25. Creaven, B.S., Donlon, D.F., and McGinley, J., *Coord. Chem. Rev.*, 2009, vol. 253, no. 7, p. 893.
26. Bi, Y., Du, S., and Liao, W., *Coord. Chem. Rev.*, 2014, vol. 276, p. 61.
27. Yuan, D., Wu, M., Wu, B., et al., *Cryst. Growth Des.*, 2006, vol. 6, no. 2, p. 514.
28. Ishii, Y., Takenaka, Y., and Konishi, K., *Angew. Chem. Int. Ed.*, 2004, vol. 43, no. 20, p. 2702.
29. Hoppe, E. and Limberg, C., *Chem. Eur. J.*, 2007, vol. 13, no. 24, p. 7006.
30. Sheldrick, G.M., *SHELXS2014*, University of Göttingen, Germany, 1997.
31. Sheldrick, G.M., *SHELXL2014*, University of Göttingen, Germany, 1997.
32. Barron, P.F., Dyason, J.C., and Healy, P.C., *Dalton Trans.*, 1986, nos. 1965–1970, p. 1965.